DrainScope: Visual Analytics of Urban Drainage System

Mingwei Lin, Zikun Deng, Qin Huang, Yiyi Ma, Lin-Ping Yuan, Jie Bao, Yu Zheng, and Yi Cai

***Abstract*—Urban drainage systems, often designed for outdated rainfall assumptions, are increasingly unable to cope with extreme rainfall events. This leads to flooding, infrastructure damage, and economic losses, necessitating effective diagnostic and improvement strategies. In current practice, conventional analysis platforms built on hydrological–hydraulic models provide only limited analytical support, making it difficult to pinpoint defects, inspect causal mechanisms, or evaluate alternative design options in an integrated manner. In this paper, we develop DrainScope, to our knowledge, the first visual analytics approach for comprehensive diagnosis and iterative improvement of urban drainage systems. Defects are initially observed in the map view, after which DrainScope extracts the critical sub-systems associated with them using a rule-based search strategy, enabling focused analysis. It introduces a novel drainage-oriented Sankey diagram to visualize internal flow dynamics within the focused, static drainage system, revealing the causes of identified system defects. Furthermore, it enables flexible modification of drainage components corresponding to identified defects, coupled with a comparison view for rapid, iterative evaluation of improvement plans. We evaluate DrainScope through a real-world case study and positive feedback collected from domain experts.**

***Index Terms*—Urban visual analytics, urban drainage system, causal analysis.**

I. Introduction

THE frequency of urban flooding events has risen sharply worldwide due to increasingly extreme rainfall, leading to significant economic losses, infrastructure damage, and human casualties [1]–[3]. Urban drainage systems play a vital role in mitigating urban flooding by efficiently collecting, conveying, and discharging stormwater. However, many existing drainage systems were designed based on historical rainfall patterns, making them increasingly ill-equipped to handle intensifying hydrometeorological extremes. A comprehensive analysis of urban drainage systems can help identify critical components that contribute to urban flooding [4], [5]. This analysis facilitates targeted interventions and informs infrastructure optimization, enhancing city resilience.

Experts often utilize hydrological-hydraulic models to analyze urban drainage systems. These models simulate the hydrodynamic behavior of drainage systems under varying rainfall conditions and generate numerical outputs [6]–[8], for example, flow volume within systems. Such outputs can be used to identify system defects (i.e., the components prone to causing flooding). However, they lack causal context and therefore provide limited insight into the underlying causes of system defects. For example, when flooding is observed in a certain region, it is difficult to determine whether it is caused by excessive upstream inflow, downstream congestion, or backward flow. This lack of causal clarity requires experts to manually examine simulation outputs across time and space, using domain expertise to infer the contributing factors. This process is both time- and labor-intensive, and lacks a standardized framework for analysis. In addition, improving drainage systems is an iterative process that involves repeated adjustments and evaluations of previous design plans. Existing drainage analysis platforms [9], [10] typically offer limited interactive support for iterative improvement, limiting the ability of users to efficiently evaluate multiple design plans.

These aforementioned limitations motivate us to propose a visual analytics approach that leverages interactive, causality-oriented visual representations to assist experts in analyzing and improving urban drainage systems. However, developing such an approach is challenging due to:

Large-scale and complex drainage system. An urban drainage system can be abstracted as a network typically consisting of hundreds of nodes and pipelines, making manual inspection and analysis of system defects particularly challenging. Moreover, once a system defect is identified, determining which components of the system have a potential impact on it adds another layer of complexity. An efficient approach is essential to help users quickly identify system defects and the relevant sections of the network that contribute to them, which we refer to as *the relevant sub-system*.

Multi-factor causal analysis for drainage processes. Analyzing the causes of system defects requires considering both the static structure of the drainage sub-system and the dynamic behavior of water flows, such as their direction, volume, and confluence. For example, *is there excess water flowing into the under-capacity pipelines?* For such multi-factor causal

The work was supported by the National Natural Science Foundation of China (62402184), Fundamental Research Funds for the Central Universities (226-2024-00033), Guangdong Basic and Applied Basic Research Foundation (2025A1515010162), Guangdong Provincial Fund for Basic and Applied Basic Research—Regional Joint Fund Project (Key Project) (2023B1515120078), Guangdong Provincial Natural Science Foundation for Outstanding Youth Team Project (2024B1515040010), and Science and Technology Planning Project of Guangdong Province (2025B0101120003). Z. Deng is the corresponding author.

M. Lin, Z. Deng, Q. Huang, and Y. Cai are with the School of Software Engineering, South China University of Technology and Key Laboratory of Big Data and Intelligent Robot (SCUT), Ministry of Education. Z. Deng is also with the State Key Laboratory of Subtropical Building and Urban Science. Emails: ptlmw666@gmail.com; zkdeng@scut.edu.cn; h2513561399@gmail.com; ycai@scut.edu.cn.

Y. Ma is with the College of Civil Engineering and Architecture, Zhejiang University. Email: yiyima@zju.edu.cn.

L.-P. Yuan is with the Hong Kong University of Science and Technology. Email: yuanlp@ust.hk.

J. Bao and Y. Zheng are with JD Intelligent Cities Research. Emails: baojie@jd.com; msyuzheng@outlook.com;

Manuscript received April 19, 2021; revised August 16, 2021.

analyses, an effective visualization approach is required to integrate the key sub-system with its internal flow dynamics, enabling experts to efficiently identify anomalous flow patterns and pinpoint the causes of system defects.

Flexible, iterative improvement of the drainage system. To address identified defects, users must be able to propose modifications to the urban drainage system. As improvement is an inherently iterative process, multiple modifications are often necessary to achieve effective plans. In this context, it is crucial to provide intuitive and flexible interaction mechanisms for implementing changes. Besides, both tracking multiple proposed improvement plans and comparing their performance are essential to facilitate informed decision-making.

To address these challenges, we propose DrainScope, a visual analytics approach for analyzing and improving drainage systems. For the first challenge, we extract sub-systems potentially responsible for defects by applying a rule-based search to simulation results generated from rainfall data and the abstracted drainage system. In this way, users can focus on analyzing key parts of the drainage system. For the second challenge, we refine the layout of the Sankey diagram to not only illustrate internal flow dynamics within the sub-system but also intuitively convey the relative elevation differences and topological relationships among the components within the sub-system. This novel visualization approach enables experts to easily discern anomalous water flowing patterns and pinpoint the root causes of defects. For the third challenge, we implement flexible user interactions for modifying the urban drainage system and design a comparison view to track, roll back, and evaluate these modifications. These features enable users to efficiently navigate and refine drainage system modifications over multiple iterations. We present a case study on a real-world urban drainage system that demonstrates DrainScope's effectiveness. We also conduct expert interviews, where positive feedback and suggestions are collected.

Our main contributions are summarized as follows: **(1)** We characterize the domain problem of urban drainage system analysis following a three-step decision-making framework; **(2)** We design a drainage-oriented Sankey diagram, coupled with an automated extraction of the relevant drainage sub-system, to visualize the drainage process for system defect causality reasoning; **(3)** We develop DrainScope (https://github.com/Ptlmv/DrainScope), a novel visual analytics approach that assists experts in effectively identifying critical system defects, reasoning their root causes, and improving the drainage system. To the best of our knowledge, it is the first visual analytics approach for urban drainage systems; **(4)** We evaluate the feasibility and effectiveness of DrainScope through a case study and expert interviews.

II. Related Work

A. Urban Drainage System Analysis

In recent years, extreme weather events have become increasingly frequent [1]. In particular, the occurrence of heavy rainfall events has repeatedly challenged urban drainage systems, leading to significant material and economic losses [2], [3]. The analysis of urban drainage systems has become an important research field in both the academic and engineering communities worldwide [4], [5]. Urban drainage system analysis can be categorized into *hydrological-hydraulic* approaches [6], [7] and *machine learning-based* approaches [8].

Hydrological-hydraulic approaches integrate hydrological processes (e.g., rainfall-runoff simulation) with hydraulic processes (e.g., flow dynamics within drainage networks), providing comprehensive insights into system performance under various rainfall scenarios, as demonstrated in the approaches of Chang et al. [11] and Khatooni et al. [12]. Two of the most widely used models in this domain are the Storm Water Management Model (SWMM) and the Infoworks Integrated Catchment Management model (Infoworks ICM), each implemented in corresponding platforms bearing the same names.

SWMM is frequently applied to simulate the hydrological and hydraulic behaviors of small to medium-sized urban drainage systems, owing to its flexibility and robust interactive features [9], [10], [13]. This model facilitates a detailed evaluation of runoff dynamics and the performance of drainage networks under varying rainfall scenarios. In our study, SWMM is used to simulate the drainage system behavior under varying rainfall conditions. Notably, as a piece of open-source software, SWMM enables users to customize the model or integrate it with other models to meet a broad range of research needs [12], [14]. In contrast, the Infoworks ICM model is typically employed for analyzing large-scale and complex urban drainage systems, benefiting from its advanced two-dimensional hydrodynamic modeling and non-linear flow processing capabilities [15], [16]. These features allow for more precise simulations, particularly in intricate urban environments. However, Infoworks ICM requires a paid license and lacks the open-source flexibility provided by SWMM.

Machine learning-based approaches have gained increasing attention in recent years for urban drainage system analysis [17]. These techniques improved the prediction of drainage system performance and can be used to optimize design, operation, and maintenance, advancing the management of urban drainage networks. For instance, Hosseniny et al. [18] proposed a novel hybrid model combining hydraulic simulation with an artificial neural network, demonstrating superior computational efficiency and accuracy in identifying flood extents and depths. Yin et al. [19] introduced a defect detection system based on a deep convolutional neural network, designed for analyzing sewer pipelines monitored via closed-circuit television footage. Noymanee et al. [20] integrated a hydrological forecasting model with machine learning models for flood level prediction and early warning.

Despite advancements, existing approaches remain limited in several key aspects. Primarily, these approaches are capable of detecting defect points within the drainage system, such as abnormal discharge occurring at drainage nodes, but they often fail to pinpoint the underlying causes of these issues. Prior visualization efforts have aimed to improve the interpretability of simulation results, for example, by offering dynamic 3D displays of the entire drainage process [21] or by mapping vulnerabilities onto 3D building models [22]. However, these approaches mainly emphasize what is happening, offering limited support for exploring why it occurs. To address this

gap, we combine the popular SWMM model with interactive visualizations to facilitate explainable discovery, causal analysis, and optimization of drainage system defects.

B. Urban Visual Analytics

Due to the effectiveness of modern urban data visualization and analytics techniques [23]–[25], urban visual analytics has been widely applied across various fields, such as transportation [26], environmental science [27], architecture [28], and public services [29]. Deng et al. [30] categorized urban visual analytics approaches into two broad areas: *urban visual diagnosis* and *urban visual planning*.

Urban visual diagnosis focuses on uncovering patterns within complex, dynamic urban data, such as mobility [31], co-occurrence [32], correlations [33], urban performance [34], road network centrality [35], and urban flooding [36]. Key methods related to our study include defect detection and spatial propagation analysis.

For defect detection, Deng et al. [37] visualized multimodal trajectories to identify flaws in transportation systems. Zanabria et al. [38] combined hotspot detection with tailored visualizations to analyze street-level crime patterns. Besides, Cao et al. [39] introduced a visual analytics system designed to detect anomalies in multidimensional urban data. In the field of urban flood analysis, which is closely related to this study, Rauer-Zechmeister et al. [40] employed color encoding to visualize flood risks for each building, aiding the identification of vulnerable buildings. Cornel et al. [41] introduced uncertainty-aware visualizations to reveal which flood scenarios pose the greatest threat to target buildings.

For spatial propagation analysis, Deng et al. [42] detected and visualized cascading urban event patterns using a geo-network structure. Similarly, Deng et al. [43] extracted and visualized the air pollution propagation paths with sufficient frequency. Causal analysis is also a popular method to extract propagation patterns. Deng et al. [30] applied visual causality analysis to detect causal pathways of urban phenomena. Jung et al. [44] focused on traffic congestion propagation through Granger causality, while Pi et al. [45] explored the same topic using traffic flow theory.

However, to the best of our knowledge, visual diagnosis of urban drainage systems is still an unstudied problem. The urban drainage process is affected by factors such as topography, rainfall, pipe topology, and backflow, making existing methods inapplicable. In this study, we propose the first visual analytics approach for urban drainage systems.

Urban visual planning primarily aids urban managers and experts in decision-making during urban development, such as route planning [46]–[48] and location selection for important facilities [29], [49], [50].

For route planning, Weng et al. [51] developed the BNVA system, a visual analytics tool for public transportation networks, which helps transit planners analyze and optimize bus route networks. Deng et al. [26] developed TraSculptor, designed for iterative modification of the road network and comparison of multiple road networks.

For location selection, Liu et al. [52] introduced a visual analytics system, SmartAdP, designed to assist billboard planners in selecting the most suitable billboard locations. Zhang et al. [53] proposed the CSLens system, helping planners make informed decisions regarding the deployment of charging infrastructure within the context of coupled transportation and power networks. Urban visual planning also has many applications in the field of urban flood analysis. For example, Ribičić et al. [54] enabled experts to analyze flood simulation results with different barrier configurations for informed flood control. Waser et al. [55] developed an interactive tool that helps manage the complex simulation iterations and find effective countermeasures for urban flooding.

Our proposed visual analytics approach will support drainage system planning with what-if analysis by integrating drainage system modification, real-time drainage simulation, and result comparison. Different from Ribičić et al.'s and Waser et al.'s studies, we attempt to reduce urban flood damage through improving drainage systems rather than the placement of ground barriers.

III. Background

In this section, we introduce key concepts of an urban drainage system, the SWMM model for simulating the urban drainage system, the design process of our approach, and finally, the requirements gathered from domain experts.

A. Concepts

We first formally introduce key concepts used in this paper.

An **urban drainage system** is an infrastructure network designed to collect, convey, and regulate rainwater in urban areas. Its primary functions include preventing flooding, mitigating waterlogging, and reducing surface runoff to minimize environmental impacts. It is usually modeled as a directed graph $G = (V, E)$. Each vertex $v_i \in V$ represents a drainage node with a geographic location. There are two main types of drainage nodes, namely, surface *catchments* and underground *junctions*. Each directed edge $e_i \in E$ is a drainage pipeline that establishes hydraulic connections between two nodes, showing flow conveyance within the network. There are two main types of drainage pipelines, namely, *ditches* and *conduits*. Formally, an urban drainage system comprises four fundamental components: *catchments*, *junctions*, *ditches*, and *conduits* (Fig. 1A).

- **Catchments** delineate surface drainage areas, such as rooftops, impervious pavements, and pervious green spaces, which intercept rainfall and govern key hydrological processes, including infiltration and runoff generation. Each catchment possesses three static attributes, *surface roughness*, *slope*, and *impervious area percentage*, as well as a dynamic attribute, *runoff*. These static attributes describe the topographic characteristics of the catchment. Impervious area percentage refers to the proportion of a catchment's surface that is covered by impermeable materials, such as concrete or asphalt, which prevent water infiltration and increase surface runoff. The runoff represents the volume of surface runoff produced over a

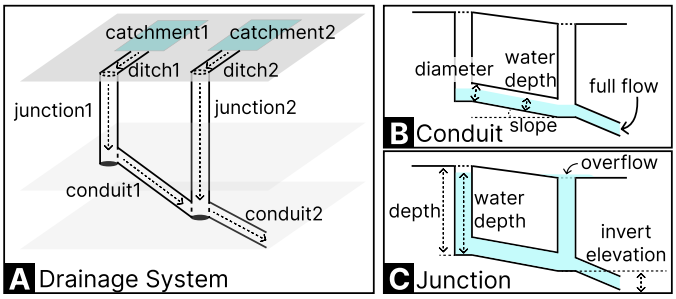

Fig. 1. (A) An urban drainage system consists of four kinds of components: catchments and ditches on the surface, and junctions and conduits underground. (B) A conduit has two static attributes, slope and diameter, both of which determine the drainage capacity. A conduit reaches full flow conditions when the water depth equals its diameter. (C) A junction has two static attributes: invert elevation and depth. When the water in the junction exceeds its depth, overflow occurs.

given time interval, which is affected by these characteristics. This runoff is directed through drainage ditches into the corresponding underground junctions.

- **Junctions** (Fig. 1C) receive water flow from upstream junctions or surface catchments and transmit it to downstream junctions. Each junction has two static attributes, *invert elevation*, and *depth*, and three dynamic attributes, *water depth*, *inflow*, and *outflow*. The invert elevation indicates the height of the junction's bottom relative to sea level. The depth attribute is the maximum allowable water depth in the junction, while water depth denotes the actual water depth at a given moment. Inflow and outflow refer to the total volumes of water entering and leaving a junction within a given time interval, respectively.
- **Ditches** are pipelines between surface catchments and the underground drainage system, allowing surface runoff to enter the underground system. The drainage capacity of ditches is generally assumed to be unrestricted.
- **Conduits** (Fig. 1B) form hydraulic connections between junctions at varying elevations, facilitating gravity-driven water flow from higher to lower terrain. Each conduit is a circular pipeline characterized by two static attributes, *slope* and *diameter*, and two dynamic attributes, *water depth* and *discharge*. The slope is determined by the elevation difference between the two ends of the conduit and the geographic distance between them, which influences flow velocity in the conduit. The diameter represents the maximum allowable water depth within the conduit, while water depth denotes the actual water depth at a given moment. The discharge refers to the total volume of water flowing through the conduit over a specified time interval. A larger diameter allows for a higher maximum instantaneous discharge, whereas an insufficient diameter can restrict drainage from upstream.

Collectively, these components form a network that allows simulation of urban drainage dynamics, including rainfall-runoff transformation, water conveyance, and system response analysis, thereby supporting performance evaluation and infrastructure optimization. The effectiveness of a drainage system is often challenged by hydraulic anomalies that disrupt expected flow patterns and reduce drainage efficiency. Three significant anomalies that contribute to urban flooding are *junction overflow*, *conduit full flow*, and *backflow*.

- **Junction overflow** (Fig. 1C) is a critical factor that can directly trigger urban flooding. It occurs when the water depth at a junction exceeds its designed depth, causing excess water to spill onto the surface and disrupt normal drainage operations. In this work, such overflow events are treated as direct manifestations of system defects.
- **Conduit full flow** (Fig. 1B) occurs when the water depth within a conduit reaches its maximum diameter, indicating that the conduit has reached its hydraulic capacity. While full flow does not directly cause urban flooding, it imposes a significant limitation on the drainage efficiency at junctions. If a conduit remains in full flow while the inflow at its upstream junction continuously exceeds the conduit's discharge capacity, excess water will accumulate at the junction, increasing the risk of overflow.
- **Backflow** occurs when downstream water levels and pressure exceed upstream conditions, causing flow reversal from downstream junctions to upstream ones. Backflow disrupts the expected drainage pattern, exacerbates upstream water accumulation, and can ultimately contribute to junction overflow and system-wide inefficiencies.

Finally, we introduce two rainfall-related concepts as the drainage simulation necessarily requires rainfall data.

- **Rainfall time series** represent the temporal distribution of rainfall intensity over a specified time span, providing a detailed profile of precipitation dynamics. Formally, a rainfall time series is a series of rainfall intensity values, typically expressed in millimeters per unit time (e.g., mm/h), recorded at regular intervals.
- **Rainfall events** are defined as distinct periods of precipitation, characterized by their duration, intensity, and total accumulated rainfall. They enable users to pinpoint relevant time periods while filtering out drainage processes during non-significant periods. Rainfall events can be extracted from rainfall time series using a predefined rainfall intensity threshold. In this study, we utilize a dataset in which rainfall events have already been annotated.

B. SWMM Simulation

The SWMM takes a rainfall time series and the urban drainage system introduced above as input. It simulates drainage dynamics by integrating two stages: hydrological processes and hydraulic processes. In the hydrological phase, each catchment receives rainfall and partitions it into different processes, including interception, infiltration, and surface runoff generation. A portion of the rainfall is intercepted by vegetation or stored on the surface, while another portion infiltrates into the soil. The remaining excess rainfall contributes to surface runoff, whose flow velocity is influenced by surface roughness and slope and can be estimated using the Manning equation. For example, based on the rainfall time series, a catchment receives 20 m^3 of rainfall at a specific time step. Of this, 15% is intercepted by vegetation and surface storage, and 35% infiltrates into the soil. The remaining 50% generates

surface runoff, which then moves across the terrain according to local slopes and roughness conditions, with its velocity estimated using the Manning equation. The resulting runoff, serving as input to the hydraulic phase, is then routed through ditches and enters a network of junctions and conduits. The transport of water through conduits is simulated following hydraulic principles governed by the Saint-Venant equations.

In sum, the SWMM computes the dynamic attributes for the urban drainage system at each time step in the simulation process. Specifically, given a time series of rainfall and an urban drainage system, the SWMM outputs the following six kinds of time series with the same temporal granularity as the rainfall time series: (1) water depth, (2) inflow, and (3) outflow time series for every junction; (4) water depth and (5) discharge time series for every conduit; (6) surface runoff time series for every catchment.

C. Design Process

This work generally follows the nine-stage framework of design study proposed by Sedlmair et al. [56]. Below are key stages for developing and finalizing our approach:

Winnow and Cast. This project was a collaborative effort among three teams over seven months. Team A specializes in visual analytics, Team B has six years of experience in smart cities, and Team C has focused on urban drainage system analysis and optimization for more than five years. The project was initiated by Team B, after which Team A invited Team C to join and delegated personnel to acquire domain knowledge on urban drainage systems from Team C. Each team contributed distinct expertise to problem framing, system design, and validation.

Discover. A primary concern in urban drainage system analysis is the occurrence of overflows, which arise when stormwater cannot be effectively discharged through the drainage system into the subsurface, rivers, or seas. When this happens, excess water overflows through junctions, increasing the likelihood of urban flooding, causing economic damage, and posing significant risks to infrastructure and public safety. Therefore, improving urban drainage systems involves identifying overflow events (where), analyzing their underlying causes (why), and proposing effective mitigation strategies (how) to ultimately reduce the frequency and severity of overflows.

Design, Implement, and Deploy. Based on the characterized domain problems, Teams A and B collaboratively developed a series of visualization prototypes. Team A was responsible for implementing the visualization and interaction modules, while Team B contributed data processing strategies and algorithmic ideas, which were then implemented by Team A. These prototypes were refined through an iterative design process. A graduate student from Team A (S1), who had a background in visual analytics and gained domain knowledge through collaboration with Team C, regularly demonstrated the evolving prototypes to two domain experts: E1, a senior smart city specialist from Team B, and E2, a professor from Team C with over ten years of research experience in urban drainage systems. This iterative refinement not only improved the visual design but also helped refine requirements and strengthen the teams' understanding of domain-specific challenges.

D. Requirements

The derived requirements can be structured following the well-established decision-making framework: Intelligence, Design, and Choice [57].

Intelligence. The first stage involves identifying and understanding overflow occurrences within the drainage system:

- **R1: Identification of overflow events**, pinpointing locations where stormwater tends to exceed system capacity and overflows frequently occur. Experts emphasized that limited resources should be strategically directed to these critical locations to optimize system performance and support informed decisions. Satisfying this requirement calls for spatiotemporal visual analysis of simulation data, providing **(R1.1)** an overview of drainage system behavior by depicting overflow frequencies at underground junctions, complemented by waterlogging frequencies at surface catchments and full flow frequencies at pipelines. Moreover, the system should support (**R1.2**) narrowing the spatial scope from the entire city to specific areas of interest, and (**R1.3**) the temporal scope from extended simulation periods to critical time windows. This progressive focusing enables experts to conduct follow-up analysis based on specific severe overflow events.
- **R2: Causal analysis of overflows**, examining hydraulic and structural factors that contribute to overflow formation. Overflows frequently arise due to the inability of static drainage infrastructure to accommodate dynamic water flows. For example, a shallow junction may lack sufficient storage capacity, leading to rapid overflow, or excessive inflow into a conduit with a limited diameter may exceed its discharge capacity. Effective causal analysis necessitates not only the representation of static drainage attributes, such as topography and expected flow direction, but also the visualization of dynamic processes, such as water movement, volume accumulation within conduits and junctions. To support such analysis, the system should integrate (**R2.1**) static infrastructure and (**R2.2**) dynamic flow behaviors into a unified visual representation, enabling experts to trace overflow causes and understand their spatiotemporal patterns.

Design. Once the underlying causes are understood, the next step focuses on designing mitigation strategies:

- **R3: Improvement of drainage capacity**, encompassing infrastructure modifications and drainage rerouting strategies to enhance system resilience. For instance, increasing conduit diameters in high-risk areas can mitigate overflows during extreme rainfall events, while redirecting excess water to lower-risk areas may achieve similar effects. To support effective improvement, the system should provide (**R3.1**) intuitive interactions that allow experts to modify and extend the existing drainage system efficiently, such as adjusting conduit diameters or increasing green space. It should also support (**R3.2**) integrated simulation, enabling experts to assess the impact of these changes within a coherent analytical context.

Choice. The final stage involves evaluating alternative improvement plans to support informed decision-making:

- **R4: Comparative evaluation of improvement plans,** evaluating their effectiveness within the drainage system. In practice, experts often iteratively generate multiple plans, evaluate their differences, and ultimately select the one that best meets the system objectives. This process typically involves comparing the plans' effectiveness, such as assessing which plan more significantly reduces overflow severity in affected regions by visually contrasting pre- and post-improvement conditions across the regions. In addition, it is important to reveal the inheritance relationships among the plans, enabling experts to understand how each plan evolves from previous versions. Therefore, the system should provide a comparative visualization that not only enables (**R4.1**) intuitive comparison across multiple improvement plans but also preserves and communicates (**R4.2**) their inheritance structure throughout the iterative design process.

IV. DrainScope

This section introduces the system design of DrainScope, including the visualization and interactions.

A. System Overview and Workflow

To meet the domain requirements, we developed DrainScope, a visual analytics system designed to assist experts in analyzing and improving urban drainage systems based on SWMM simulations. It integrates three coordinated views to support an interactive and iterative workflow, aligning with the visual analytics principle "overview first, zoom and filter, then details-on-demand" [58].

Users begin with the map view (Fig. 3A), where component-level indicators are visualized to highlight regions prone to system defects (**R1.1**). These indicators are aggregated from SWMM simulations of historical rainfall events, which are conducted in advance and serve as the primary data source throughout the exploration process. Users can then narrow the spatial scope to a region of interest (**R1.2**). Once a target region is selected, the analysis view (Fig. 3B) automatically recommends the severe rainfall events that reflect typical overflow conditions within the region (**R1.3**). Users select one of these events and explore individual junctions using a drainage-oriented Sankey diagram, which is derived through a sub-system extraction method applied to the SWMM simulation results of the selected event. This diagram integrates both the static infrastructure (**R2.1**) and the dynamic flow behaviors (**R2.2**), enabling detailed causal analysis. Based on these insights, users can apply targeted modifications directly in the map view (**R3.1**), after which the system is resimulated using SWMM under the same rainfall event (**R3.2**). The comparison view then adds a new bar representing the overflow severity derived from the updated simulation. Selecting this bar updates both the map and analysis views to reflect the corresponding simulation state, enabling further exploration and refinement. Moreover, the comparison view (Fig. 3C) supports visual comparison of simulation results (**R4.1**) and reveals the inheritance relationships among improvement plans (**R4.2**) to evaluate and manage multiple improvement plans. If the result of a given plan is unsatisfactory, users can revert to previous versions and initiate a new improvement cycle until a suitable solution is identified (**R3.1**, **R3.2**).

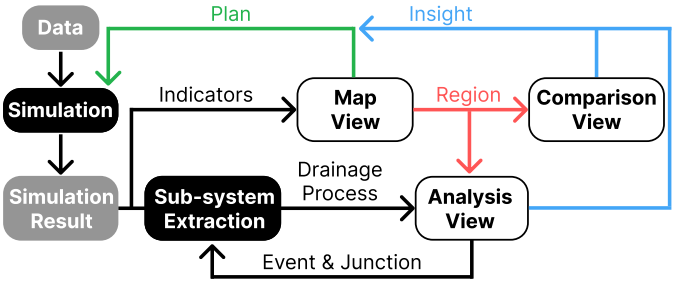

Fig. 2. System architecture. The gray blocks denote the data storage at the backend. The black blocks are computational modules running at the backend. The white blocks are visualization modules running at the frontend.

DrainScope is a web-based application designed to run on modern browsers (Fig. 2). It follows a client-server architecture, consisting of a backend for simulation processing and a frontend for interactive visualization. The backend, implemented in Python, interfaces with the SWMM engine through the *PySWMM* API to trigger simulations and store simulation results, including six types of time series data. It loads pre-computed simulation results for historical rainfall events to derive overview indicators, and performs on-demand resimulations when users modify the drainage system. Beyond simulation, the backend also hosts a sub-system extraction module, which identifies drainage components contributing to overflows, facilitating users to investigate their root causes. The frontend, developed in TypeScript using the Vue 3 framework, provides interactive visualizations across the map, analysis, and comparison views. Most visual elements are implemented using D3.js, while the geospatial context in the map view is rendered with Leaflet.js. These visual interfaces support users in analyzing simulation results, identifying overflow-prone junctions, reasoning about their causes, and optimizing drainage performance.

All development and testing were conducted on a desktop system running Windows 11, equipped with an Intel Core i7-13700K 3.40 GHz CPU and 32 GB of RAM. For a 12-hour rainfall event with a 1-minute temporal resolution, simulating a drainage system consisting of 713 catchments, 1020 junctions, 713 ditches, and 1044 conduits takes approximately one minute on this configuration. This demonstrates that DrainScope can efficiently support iterative scenario testing and refinement even on standard personal computing hardware.

B. Map View

The map view (Fig. 3A) presents the overall structure of the drainage system, integrating statistical indicators to highlight system defects for identifying overflow-prone junctions (**R1.1**). In addition, the map view provides intuitive interactions that allow users to modify the topology and the properties of components within the drainage system (**R3.1**), and resimulate (**R3.2**) to enhance its drainage capacity.

We adopt a 2D map instead of a 3D representation that includes terrain and building elevations primarily to reduce

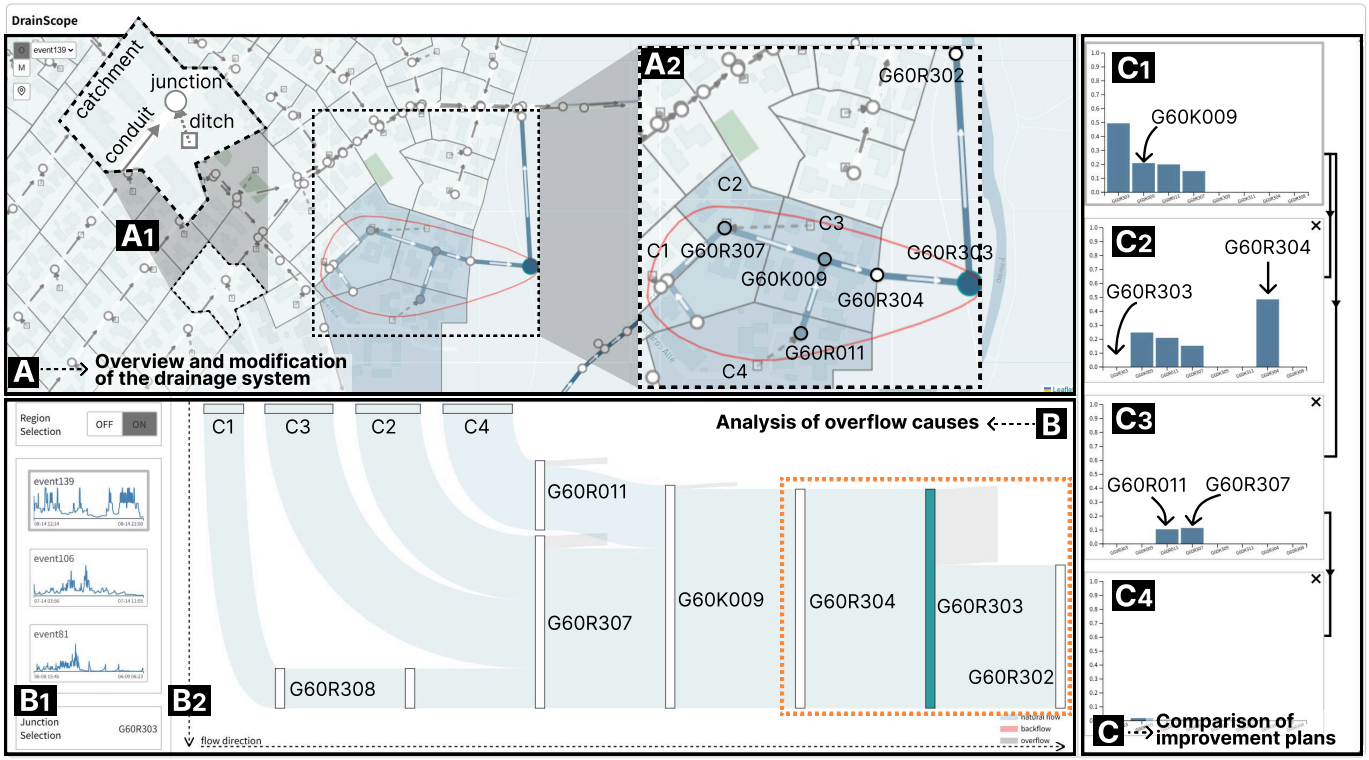

Fig. 3. The system interface of DrainScope. (A) The map view displays the drainage system topology with (A_1) its four components and visually presents system defects. It enables users to directly modify the topology and the properties of these components. (B) The analysis view comprises (B_1) a configuration panel for specifying study targets and (B_2) a drainage-oriented Sankey diagram for analyzing overflow causes. (C) The comparison view presents a set of bar charts to visually compare overflow conditions across different drainage system configurations, including the original (C_1) and the improvement plans (C_2, C_3, and C_4), enabling users to make informed decisions based on comparative analysis.

visual occlusion commonly encountered in 3D environments. Notably, variables such as flow velocity and elevation have already been accounted for in the SWMM simulation process. In user analysis, elevation information primarily serves to infer flow direction, as water flows from higher to lower elevations. To support this analytical need, we explicitly encode flow direction in the visualization by placing directional arrows along the pipelines (see details below).

1) Visualizing the Drainage System: **Indicators.** Before visualization, the drainage system is simulated using SWMM under a series of rainfall events. For each event, we perform a statistical analysis of the simulation outputs to extract three key indicators. Specifically, (1) *the frequency of overflow* at each junction is calculated as the ratio of timestamps when the water depth exceeds the junction's depth to the whole timestamps. For each conduit, (2) *the frequency of full flow* is calculated as the ratio of timestamps when the water depth equals the conduit's diameter to the whole timestamps. To intuitively capture the spatial extent of junction overflow impacts, we assess the occurrence of localized surface flooding within each catchment. (3) *The frequency of waterlogging* is equivalent to the frequency of overflow at the corresponding junction, as surface water accumulation is primarily driven by overflow events at the nearest connected junction. To characterize overall drainage performance, weighted averages of these indicators are also calculated across all events, reflecting the system's long-term behavior across historical rainfall scenarios.

Visual Encodings. We adopt a geographic map to provide the spatial context. The four components of an urban drainage system are visualized as follows (Fig. $3A_1$). First, catchments are visualized as polygons on the map based on their geographical boundaries, showing their spatial coverage and distribution. Given the potential overlap of polygons with other components, a small square is placed at the center of each polygon to provide a concise representation of the catchment. We encode the frequency of waterlogging in each catchment with the polygon's color, with a darker shade indicating a higher frequency of waterlogging and vice versa. Second, junctions are depicted as circles positioned according to their geographic coordinates. The color of each circle encodes the frequency of overflows that occurred at the junction. When the zoom level is below a certain threshold (15 in our implementation), we additionally encode the frequency with circle size. Junctions with higher risks appear more prominent, while lower-risk junctions are deemphasized. Third, ditches are visualized as dashed lines between catchments and junctions. Finally, conduits are depicted using solid lines between junctions, where the color gradient denotes the frequency of full flow in the conduit. Arrows are superimposed along all ditches and conduits to explicitly show the expected flow direction according to the elevation information.

2) Modifying the Drainage System: Junction overflow serves as a critical indicator of hydraulic constraints in urban drainage systems, emerging when the inflow to a junction

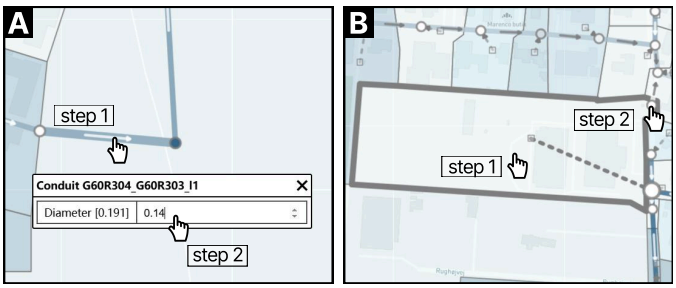

Fig. 4. The interactions for modifying the drainage system. (A) The user can modify the conduit diameter by clicking the conduit, opening the property panel, and entering the desired value. (B) The user can reroute the runoff of a catchment by first double-clicking the catchment and then clicking an alternative junction as the new outlet.

substantially exceeds its outflow capacity. The inflow of a junction is sourced from the catchment and upstream junctions, both conveyed via pipelines, while outflow is discharged through downstream conduits to the subsequent junctions. In real-world applications, numerous interventions can be employed to reduce inflow or enhance outflow, thereby alleviating overflow risks. However, it is impractical to enumerate them all. In collaboration with domain experts, we distilled three representative modifications, denoted as **M1** to **M3**.

M1: Adjusting the conduit diameter. For a junction with frequent overflows, adjusting the diameter of its connecting conduits helps balance its inflow and outflow. Specifically, reducing the diameter of its upstream conduits can limit the flow from upstream junctions, while increasing the diameter of its downstream conduits can enhance the outflow capacity. To issue this modification, users can click to select a conduit to access its property panel, and modify the diameter of the conduit by inputting a new value via the keyboard (Fig. 4A).

M2: Rerouting the flow path. In scenarios where junctions become overloaded due to excessive runoff from a catchment or inflow from upstream, while adjacent junctions retain surplus drainage capacity, flow rerouting offers a strategy to relieve system stress. By rerouting flow to the section with greater hydraulic capacity, the overall hydraulic load can be balanced, reducing the overflow risks and improving drainage efficiency. Flow rerouting is implemented by modifying the topology of the urban drainage system. To reroute the runoff of a catchment, users can double-click the catchment. The associated ditch and its downstream junction will be highlighted. Subsequently, users click an alternative junction as the new junction, allowing the runoff of the catchment to be rerouted (Fig. 4B). To reroute the outflow of a junction, the user can perform the same interaction on the junction.

M3: Reducing the catchment imperviousness. When overflow is driven by excessive runoff from a catchment, reducing its impervious area percentage (i.e., increasing green space) can mitigate the problem at the source. Lower imperviousness enhances natural infiltration and surface storage, thereby reducing runoff generation. This approach reduces the inflow to the junction from the catchment, alleviating the risk of overflow. To apply this modification, users can click to select a catchment to open its property panel, and adjust the impervious area percentage by inputting a new value.

Users can apply a series of modifications before running the simulation. These modifications form an improvement plan.

C. Analysis View

The analysis view comprises a configuration panel (Fig. $3B_1$) and a novel drainage-oriented Sankey diagram (Fig. $3B_2$). The configuration panel enables users to specify the region of interest (**R1.2**), identify significant rainfall events associated with severe overflows in the selected region (**R1.3**), and select a specific overflow-prone junction for in-depth investigation. The Sankey diagram integrates the static infrastructure of the drainage network (**R2.1**) with dynamic flow behaviors characterized by flow volume and flow direction (**R2.2**), supporting the identification of the root cause of overflow at the selected junction.

1) Specifying Study Targets: The configuration panel enables users to drill down into certain system defects through a structured three-step process. First, with the "Region Selection" toggle activated, users can define a region of interest by drawing a polygon in the map view. Second, upon confirmation of the selected region, the system automatically retrieves the severe rainfall events that affected the region. These events are ranked in descending order of overall overflow risk. Users can select an event based on their interests, and the map view updates to reflect the system's status under the selected event. Specifically, the three indicators for junctions, conduits, and catchments will be re-extracted from the simulation results for the event and re-rendered in the map view. Third, to dissect the causes of overflow in the selected region, users can initiate the analysis by clicking on every critical junction, such as the junction with the most severe overflow. The causality analysis for the overflow can be performed in the Sankey diagram.

2) Analyzing Overflow Causes: Junction overflow often results from complex hydrodynamic interactions among various drainage components. Given that a drainage system typically consists of hundreds of nodes and pipelines, directly analyzing the entire system to understand overflow formation is impractical. A more effective approach is to extract a relevant sub-system that encapsulates the critical flow propagation pathways contributing to a selected overflow-prone junction, enabling a more focused analysis. Furthermore, an effective visualization approach is needed to intuitively convey the water propagation within the sub-system. Below, we introduce in detail the methodology for sub-system extraction and the visualization called drainage-oriented Sankey diagram.

Sub-system Extraction. Extracting a relevant sub-system involves the following steps: (1) Overflow period identification, (2) Influence modeling, and (3) Sub-system construction.

First, we need to find the specific time period T during which the selected junction was in an overflowing state. In other words, any drainage process during this time period was causing the overflow. T can be identified based on the water depth time series at the selected junction. Second, we need to identify which pipeline was influencing a junction. The intuition is that only pipelines that carry large enough volumes of flow have an influence. Specifically, we employ a cumulative discharge approach to compute the total flow during the

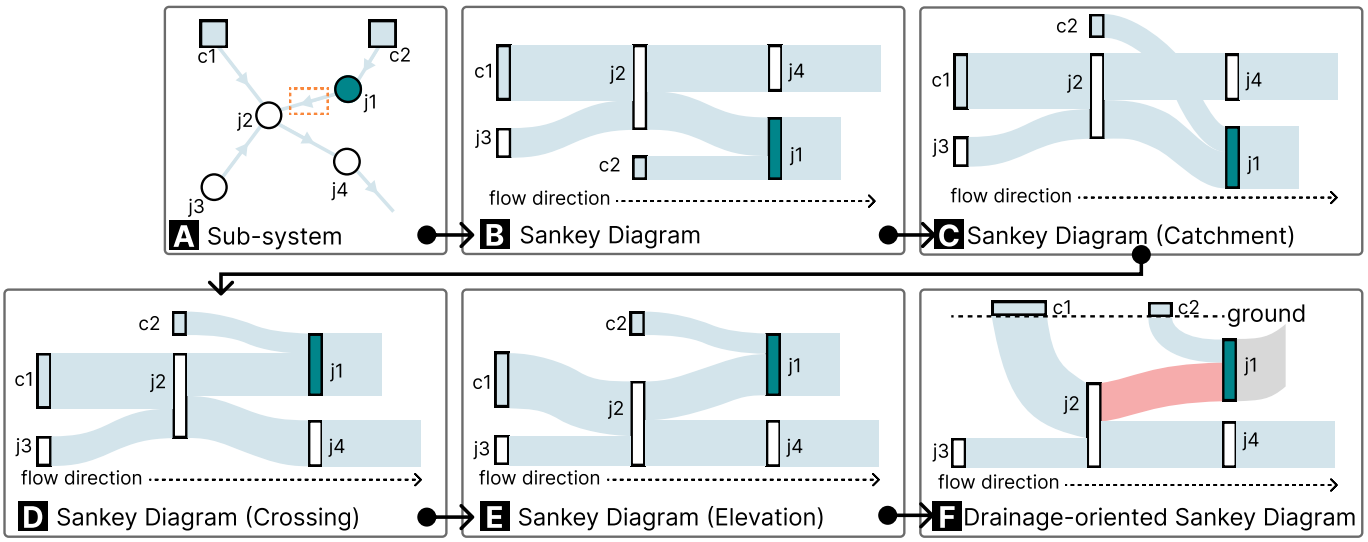

Fig. 5. Iterative design process of the drainage-oriented Sankey diagram, with (F) as the final design. (A) The sub-system that encapsulates the critical flow propagation path contributing to the selected overflow-prone junction $j1$. (B) Directly visualizing the drainage process with the Sankey diagram, where topographic context is missed. (C, D, E, and F) Layout procedure and visual encodings of the drainage-oriented Sankey diagram. (C) Catchments are placed above junctions within each layer. (D) Crossings are minimized. (E) The relative elevations between junctions in different layers are considered to reflect the expected flow direction. (F) All catchments are aligned along a common horizontal axis, with their order adjusted to improve structural clarity. Water flow is color-coded blue for natural flow, pink for backflow, and gray for overflow contributing to waterlogging.

time period T. For a conduit connecting upstream junction i to downstream junction j, its total flow $F_{i,j} = \sum_{t \in T} d(t)$, where $d(t)$ represents its discharge at time t. A positive $d(t)$ denotes flow in the conventional direction from i to j, whereas a negative $d(t)$ indicates backflow from j to i. A negative $F_{i,j}$ over the period T suggests that backflow predominates within the conduit. As ditches are not subject to discharge constraints, their flow dynamics are primarily governed by the runoff contributions from the associated catchments. Thus, for a ditch connecting catchment i to junction j, its total flow $F_{i,j} = \sum_{t \in T} r(t)$, where $r(t)$ denotes the runoff time series value from the catchment at time t. Third, we perform breadth-first searches upstream and downstream of the selected junction to construct the sub-system:

- *Downstream Search:* Traverses from the target junction downstream until encountering a conduit where $F_{i,j}$ is positive, indicating the termination of backflow.
- *Upstream Search:* Traverses upstream to identify all potential inflow sources contributing to the target junction until reaching a conduit where $F_{i,j}$ is negative, marking the boundary of upstream water contribution.

In this way, we can extract the critical sub-system where every component influenced the selected overflow-prone junction. An illustrative extracted sub-system is shown in Fig.5A, where all components influence the overflow at junction $j1$.

Drainage-oriented Sankey Diagram. The drainage process describes the flow of water in a drainage network consisting of pipelines and nodes, with the characteristics of flow volume and flow direction. The Sankey diagram is well-suited for visualizing the drainage process because it effectively represents flow volume and flow direction. The varying thickness of links intuitively depicts flow volume at different pipelines, making it easy to identify major flow paths and bottlenecks. The left-to-right arrangement emphasizes flow direction, helping to trace water movement across pipelines and nodes. Moreover, Sankey diagrams naturally support hierarchical structures and provide a clear, aggregated view of flow distribution. They also facilitate anomaly detection by allowing visual comparison of expected and actual flow proportions, helping to identify losses, blockages, or inefficiencies.

However, as shown in Fig. 5B, directly applying Sankey diagrams overlooks the elevation information, which is crucial in urban drainage analysis. First, the invert elevation of $j2$ is lower than that of $j1$ and water flowing from $j2$ to $j1$ represents an abnormal backflow. Yet, this is not visually reflected. Second, catchments and junctions are both represented as nodes without explicit differentiation. Catchments exist at the surface, whereas junctions are located underground. This lack of distinction reduces clarity in their respective hydrological roles. To this end, we propose a novel layout to integrate topographic information into the Sankey diagram and revisit the visual encodings.

The layout procedure is illustrated in Figs. 5C, D, and E. First, within each layer, we place all catchments above the junctions to distinguish catchments from junctions (Fig. 5C). For example, the catchment $c2$ is positioned above $j2$. Second, with the constraint that catchments must be placed above junctions, we apply the Sugiyama algorithm [59] to order all catchments and junctions within each layer, minimizing edge crossings and improving diagram clarity (Fig. 5D). For example, from Fig. 5C to Fig. 5D, $j1$ and $j4$ are swapped to avoid the crossing between the edge from $c2$ to $j1$ and the edge from $j2$ to $j4$. Third, we incorporate relative elevation into the vertical layout of junctions across different layers to more accurately reflect the topography-driven direction of water flow (Fig. 5E). This adjustment is performed by traversing the diagram layer by layer from left to right. For each junction

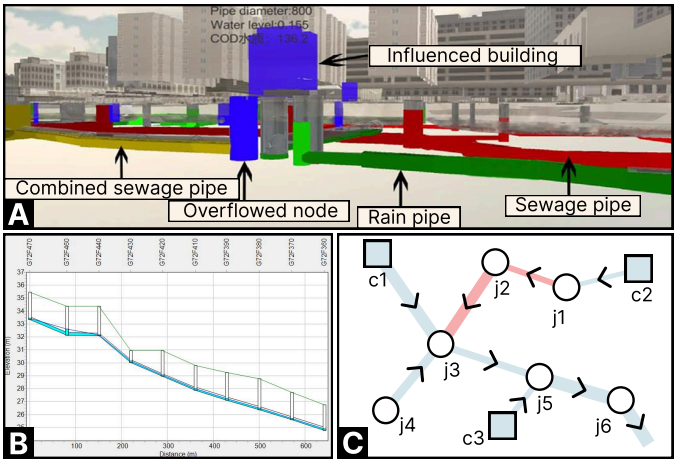

Fig. 6. Illustrations of three alternative designs for representing drainage processes: (A) 3D representations (adapted from [21]), (B) built-in visualization of the SWMM platform, and (C) node-link diagram-based visualization.

A, we adjust the vertical position of its connected junction B at the next layer based on the following rule: If A has a higher elevation than B, the bottom of B should not be higher than that of A; otherwise, the bottom of B should be placed above that of A. For example, since junction *j*3 in the first layer has a higher elevation than junction *j*2 in the next layer, we adjust the vertical position of *j*2 such that its node bottom is not higher than that of *j*3. This ensures a visual metaphor consistent with the underlying physical terrain. Finally, the catchment nodes are rotated and placed at the same horizontal level, forming the visual metaphor of the ground. Their left-to-right ordering is determined based on their original position in the Sankey diagram: catchments that were farther right and higher in the original layout are placed farther right at the highest horizontal level. Flow direction generally follows the convention, progressing from left to right and top to bottom, with color coding to enhance interpretability: blue for natural flow, pink for backflow, and gray for overflow contributing to waterlogging. Fig. 5F illustrates the final design.

Moreover, we incorporate cross-view highlighting between the Sankey diagram and the map view to facilitate spatial-contextual interpretation. When users hover over a node in the Sankey diagram, the corresponding node in the map view is highlighted; hovering over a pipeline similarly highlights the associated pipeline and its connected nodes. This design establishes a visual linkage between the abstract flow representation and the spatial topology.

Justification. We explore three alternatives, namely, 3D representations, built-in visualization of the SWMM platform, and node-link diagram-based visualizations, illustrated in Fig. 6. First, 3D representations (Fig. 6A), commonly used in digital twin applications, often suffer from severe visual occlusion, which hampers the user's ability to trace flow paths and assess system-wide behaviors. Second, the built-in visualization in SWMM (Fig. 6B) animates drainage flow along individual paths within the network. While useful for inspecting local behaviors, it lacks support for analyzing multi-source confluences and interactions across the system. Third, node-link diagrams (Fig. 6C) visualize flow volume through link width, indicate expected flow direction using arrows, and use color to denote backflow situations. However, the scattered layout of such diagrams makes it difficult to trace continuous flow processes and understand elevation-related information. In contrast, our design offers the following advantages: (1) It partially preserves elevation-related information through a tailored layout optimization strategy. (2) It reduces users' cognitive load by aggregating dynamic simulation data over a specified time window into a static, yet informative, representation. (3) Its structured left-to-right and top-to-bottom layout supports the effective encoding of additional information, such as elevation differences, flow directions, and imbalances between inflow and outflow at individual nodes, thereby making the diagram more informative for domain-specific tasks.

D. Comparison View

The comparison view (Fig. 3C) represents each improvement plan as a bar chart summarizing overflow conditions within the selected region. These charts are juxtaposed to support intuitive, quantitative comparison (**R4.1**). To facilitate tracking plan evolution, the view also incorporates visual cues indicating inheritance relationships and allows users to interactively inspect individual plans (**R4.2**).

1) Comparing Plans: **Visual Encodings.** In the bar chart, the x-axis represents individual junctions within the selected region as a nominal variable, and the y-axis indicates the overflow frequency. The first chart in this view (Fig. $3C_1$) presents the baseline scenario, which reflects system performance before any modifications. In this chart, junctions are sorted in descending order of overflow frequency to provide an overview of overflow severity across the region. When an improvement plan is implemented and the drainage system is resimulated, the comparison view automatically adds a new bar chart below the original to reflect the updated overflow conditions. By aligning the charts vertically, the system enables users to quantitatively compare overflow frequencies across different plans.

Justification. The primary criterion for decision-making is the overflow situation within the designated region. Although the Sankey diagram can reflect overflow, the design cannot be extended to the scenario of comparative analysis, no matter which of the three comparative visualization strategies [60] is adopted. Juxtaposed Sankey diagrams lack a common reference axis, hindering quantitative comparisons. Superimposing multiple Sankey diagrams further increases visual complexity, making it difficult to discern individual contributions. Explicit encoding typically relies on pairwise difference computation, which does not scale well for multiple plans.

2) Tracking Plans: **Visual Encodings.** Representing the inheritance relationships among improvement plans is essential for tracking iterative refinements. Thus, we incorporate visual cues into the comparison view. When an improvement plan is created based on an existing one, a right-side directed arrow is drawn between their corresponding bar charts to indicate their inheritance relationship (Fig. 3C).

Interactions. First of all, clicking a plan switches the system to its corresponding simulation state, allowing users

to refine the plan. If the results are unsatisfactory, users can roll back to a previous plan state or continue refining the current one, enabling flexible and interactive plan refinement. Second, building upon the visual representation, we integrate a set of highlighting functionalities into the comparison view. On the one hand, hovering over a specific bar reveals its label and overflow frequency, while simultaneously highlighting the corresponding junction in the map view to reinforce spatial association. The same junction across all bar charts is also highlighted, enhancing cross-plan comparison. On the other hand, hovering over a plan highlights the modified components in the map view, rendering them in red and showing a tooltip with their previous states, further enhancing spatial context. For instance, for the modified imperviousness, the catchment's boundary is colored red, and a message such as "*Impervious area percentage: __ to __*" is displayed.

V. Evaluation

We organized a remote workshop in which the three teams collaboratively conducted case studies. In addition to E1, Team B delegated another senior smart city expert, E3, who also has over a decade of experience in the field. Team C was represented by expert E2, along with two Ph.D. candidates and three graduate students (S2-S6), all dedicated to urban drainage research. To support collaborative exploration, DrainScope was first deployed on a cloud platform and made accessible to all participants. Before the case studies, we introduced our system, including visual encodings, user interactions, and analysis workflow. During the case study sessions, we shared our screen while operating the system, allowing participants to observe the analysis process in real time. They were encouraged to propose actions, request specific analyses, and explore the system independently using their own access. Finally, we interviewed workshop participants one-on-one to collect their feedback. Below, we first present the case study and then the feedback collected during this workshop. For clarity, in the case study section, "we" refers collectively to all workshop participants.

A. Case Study

In recent years, the rising frequency of extreme rainfall events in Denmark has intensified urban flooding, underscoring the inadequacies of current drainage systems in addressing such stressors. This case study focuses on the Bellinge drainage system in Odense, Denmark, examining the performance and optimization potential of small-town drainage systems under extreme rainfall conditions.

Data and Simulation: The dataset, originally provided by [61], includes component data for the Bellinge drainage system, rainfall time series with minute granularity in 2011, and annotated rainfall events (periods essentially) in 2011. To assess the drainage system's performance under extreme storm conditions, rainfall intensity was amplified threefold to simulate more intense rainfall scenarios. The modified rainfall data, along with the drainage system, were then integrated into the SWMM for simulations.

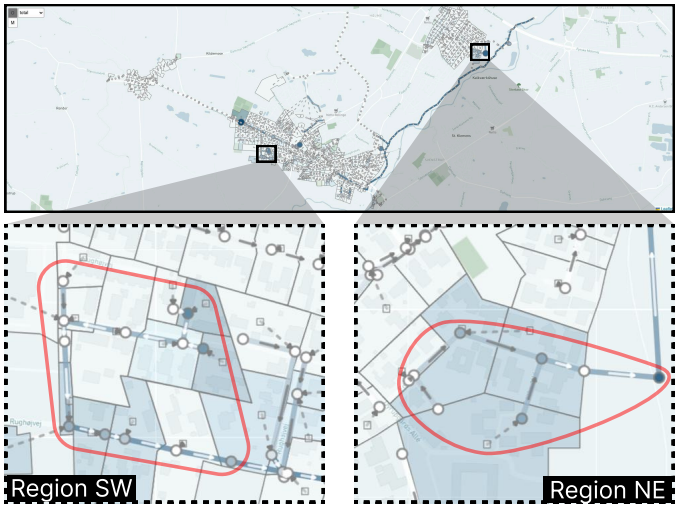

Fig. 7. The overview of the Bellinge drainage system. Regions NE and SW exhibit serious overflows, indicated by the blue circles and blue polygons.

Overview: The visual representation of the drainage system is shown in the map view (Fig. 7). We identified Region NE and Region SW, where most of the junctions exhibit darker shades, indicating a high susceptibility to junction overflow. Below, we conducted focused investigations in Region NE and Region SW. To enhance readability, each pipeline is designated using the format {*from_node*}_{*to_node*}.

1) Analysis and Improvement for Region NE: In this section, we analyzed the causes of overflows in Region NE and explored targeted improvement plans. We examined all relevant rainfall events and found that the drainage processes that caused the overflow were similar. Below, we use Event 139 as a representative event for demonstration.

As shown in Fig. $3A_2$, the conduits in Region NE frequently operated under full-flow conditions, while multiple junctions experienced overflow. Junction *G60R303* exhibited the highest severity of overflow. Therefore, we first investigated the causes of overflow at this junction. The orange dashed rectangle in the Sankey diagram (Fig. $3B_2$) showed that the inflow of *G60R303* significantly exceeds its outflow. This suggested that the drainage capacity of the system at *G60R303* was insufficient to accommodate the incoming flow, ultimately resulting in overflow. To mitigate this issue, we explored two potential optimization strategies: (1) reducing the diameter of the upstream conduit *G60R304_G60R303* to limit inflow, and (2) increasing the diameter of the downstream conduit *G60R303_G60R302* to enhance outflow.

We implemented the first improvement plan, reducing the diameter of *G60R304_G60R303* from 0.191 m to 0.14 m, and resimulated the system. The results in Fig. $3C_2$ revealed that while this modification alleviated overflow at *G60R303*, it induced adverse effects at the upstream junction *G60R304*. The diminished drainage capacity of *G60R304_G60R303* disrupted the inflow-outflow balance at *G60R304*, where inflow substantially exceeded outflow, triggering overflow. This outcome rendered the first plan ineffective.

Next, we implemented the second improvement plan by increasing the diameter of *G60R303_G60R302* from 0.18 m to

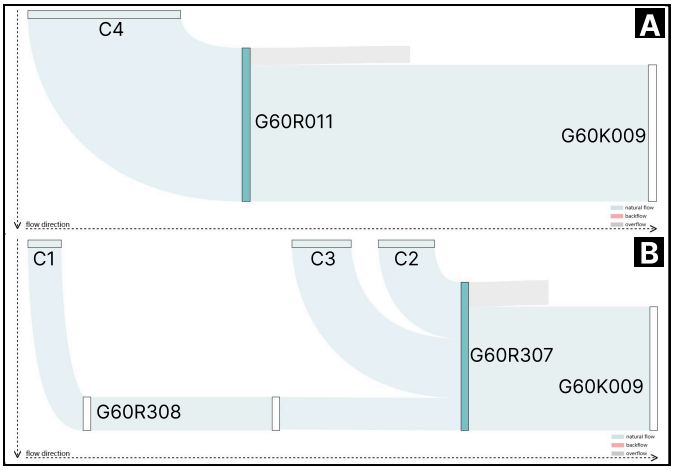

Fig. 8. Analysis of overflow mechanisms at junction (A) *G60R011* and (B) *G60R307*, respectively. (A) The inflow of *G60R011* slightly exceeds its outflow, leading to overflow at this junction. (B) A similar pattern is observed at *G60R307*, where an imbalance between inflow and outflow results in overflow at this junction.

0.26 m to enhance drainage capacity. The revised simulation results, shown in Fig. $3C_3$, demonstrated that this modification effectively alleviated overflow at *G60R303* without introducing adverse effects at other junctions. In addition, a noticeable reduction in overflow was observed at *G60K009*, likely due to the decreased water level at *G60R303*, which consequently lessened its obstructive impact on upstream drainage, highlighting the intricate interactions within the drainage system. Furthermore, minor reductions in overflow were observed at junctions *G60R011* and *G60R307*, although noticeable overflow issues persisted.

Building upon the second improvement plan, we proceeded with further refinements to address overflow at *G60R011* and *G60R307*. Analysis revealed that their overflow was primarily attributed to inadequate drainage capacity in their respective downstream conduits (Figs. 8A, B). Thus, we increased the diameters of conduits *G60R011_G60K009* and *G60R307_G60K009* to 0.21 m. To maintain flow balance at *G60K009* and *G60R304*, we also expanded the diameters of *G60K009_G60R304* and *G60R304_G60R303* to 0.21 m. Following these modifications, the overall drainage capacity in Region NE was substantially improved, with overflow incidents markedly reduced, as illustrated in Fig. $3C_4$.

Our analysis revealed a critical trade-off in drainage optimization: reducing the diameter of an upstream conduit may disrupt equilibrium at upstream junctions, whereas increasing the diameter of a downstream conduit may perturb balance at downstream junctions. This insight was affirmed by E2, stating: "*This finding captures a subtle but practically significant consideration often overlooked in engineering practice.*"

2) Analysis and Improvement for Region SW: This section investigates the overflow mechanisms in Region SW, illustrated based on Event 174, the most severe overflow event recorded in this region. The spatial distribution of overflow-prone junctions in Region SW was primarily concentrated in the upstream and downstream segments (Figs. $9A_1$, A_2).

First, we analyzed the overflows in the upstream segment. The most severe overflow was observed at junction *G73R454* (Fig. $9C_1$). The Sankey diagram analysis for this junction (Fig. $9B_1$) revealed that its sole downstream conduit, *G73R454_G73R452*, experienced backflow, which obstructed drainage at the junction and ultimately led to overflow. This backflow could be traced to the junction *G73R450*, indicating that the overflow at *G73R454* was attributable to the hydraulic anomaly at *G73R450*. Specifically, the inflow at *G73R450* exceeded its discharge capacity, causing a rise in water level that triggered the propagation of backflow, which ultimately led to overflow at *G73R454*. A similar overflow mechanism was observed at another critical junction, *G73R453*. These findings reflect a common yet often hard-to-confirm pattern in practice: upstream overflows are typically attributed to downstream bottlenecks, but pinpointing the specific component responsible is nontrivial. S2 and S3 said, "*This Sankey diagram provides a clear indication of the cause, which is extremely helpful in real-world analysis.*"

Next, we extended our analysis to the downstream segment. In this segment, junction *G73F430* experienced the highest overflow severity (Fig. $9C_1$). The Sankey diagram analysis (Fig. $9B_2$) demonstrated that its inflow surpasses its outflow, with the majority of this inflow originating from *G73R450*. This trend was consistent across other downstream junctions.

In sum, we identified *G73R450* as the primary cause of overflow in Region SW. Notably, 90% of the inflow to *G73R450* derived from runoff in catchment *C1*. To mitigate this overflow at the source, we reduced the impervious area percentage of *C1* from 0.39 to 0.15, aiming to reduce surface runoff. The resimulation results show a marked decrease in the overflow frequencies across the Region SW (Fig. $9C_2$). However, such a low level of impervious area percentage may be unrealistic under typical urban constraints, limiting the practical feasibility of this approach.

In contrast to Region SW, the adjacent Region C (Fig. $9A_3$) demonstrated superior drainage performance, with its junctions exhibiting minimal overflow and conduits rarely reaching full-flow conditions. E1 and E3 noted this discrepancy and suggested leveraging the underutilized drainage capacity of Region C as an optimization strategy to mitigate overflow in Region SW. To test this hypothesis, we proposed rerouting runoff from catchment *C1* to junction *G73F161* in Region C, rather than its original destination at *G73R450*. The distance between catchment *C1* and *G73F161* was comparable to that of *G73R450*, ensuring feasibility in terms of hydraulic conveyance. After applying the proposed modification, the simulations indicated a substantial reduction in overflow frequency across all junctions in Region SW (Fig. $9C_3$), while the drainage performance of Region C is almost unaffected (Fig. $9A_4$). These results confirmed the effectiveness of the proposed improvement plan.

B. Expert Interview

The participant feedback is summarized as follows:

Effectiveness. All three experts affirmed the effectiveness of our system, recognizing its structured workflow: overflow identification, root cause reasoning, targeted modifications,

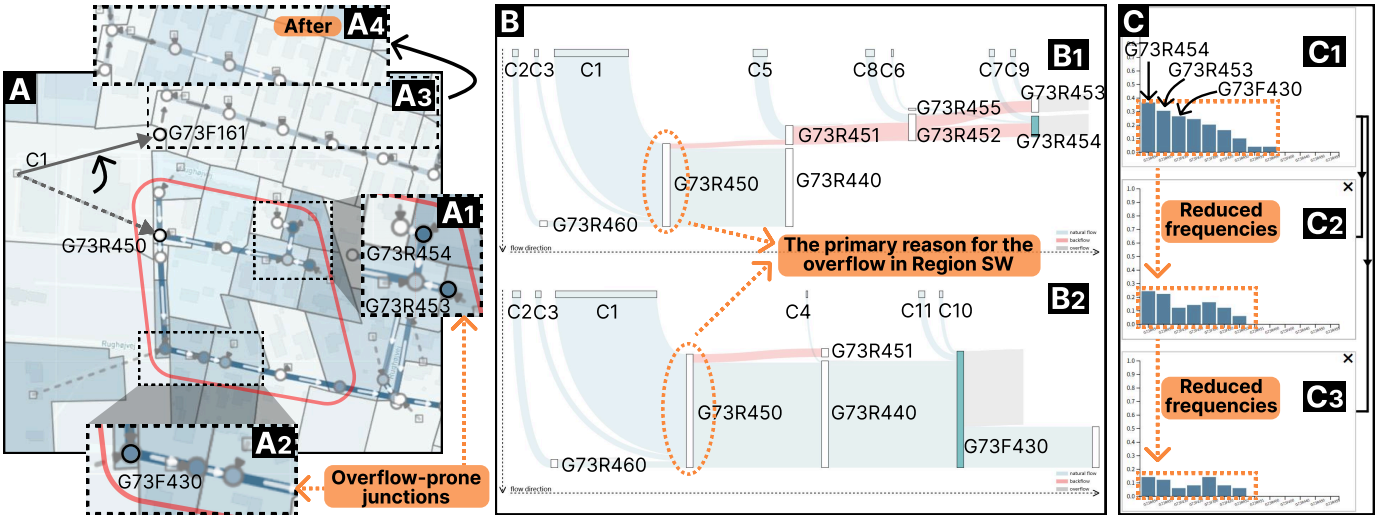

Fig. 9. Analysis and improvement of overflow conditions in Region SW. (A) The map view reveals that overflow-prone junctions are primarily concentrated along its (A_1) upstream and (A_2) downstream segments. (A_3) The adjacent Region C, situated north of Region SW, exhibits minimal junction overflow and conduit full-flow occurrences. (A_4) Region C maintains minimal overflow after system improvements. (B) Two drainage-oriented Sankey diagrams are employed to facilitate the analysis of overflow mechanisms at junctions (B_1) *G73R454* and (B_2) *G73F430*. (B_1) Severe backflow occurs along the drainage path between *G73R454* and *G73R450*. (B_1) Nearly all inflow to *G73F430* originates from *G73R450*. (C) Three bar charts illustrate overflow conditions in Region SW, showing (C_1) the baseline scenario alongside (C_2, C_3) the results of two alternative improvement plans.

and finally, evaluation and comparison. They emphasized that the system aligns well with their routine practices and enhances this familiar workflow through intuitive visualizations and interactive features that improve the clarity and efficiency of analysis. "*I believe DrainScope will be of great benefit to frontline urban drainage managers in drainage system optimization and decision making,*" underscored E2.

Visual Design. All three experts agreed that the visualizations in DrainScope are easy to learn and comprehend. They particularly appreciated the drainage-oriented Sankey diagram as it intuitively visualizes overflow mechanisms. "*The diagram clearly illustrates the topographic relationships among drainage components, making the spatial propagation of water flow within the network intuitive,* " commented E3. E1 and E2 also praised the diagram for its clarity and aesthetic appeal. This advantage can be attributed to our tailored layout strategy for the Sankey diagram, which balances topographic context with aesthetic appeal.

User Interactions. All three experts confirmed the usefulness and intuitiveness of the interactions. This positive feedback stems from several aspects of the system design, such as its intuitive way of modifying drainage systems, cross-view highlighting, and its ability to support iterative optimization, many of which represent a significant improvement over the limited interactions offered by the SWMM platform. Members in Team C commented, "*We are the first to encounter a system that allows for real-time, intuitive modifications directly on the map, with immediate visual feedback on the results.*"

Suggestions. E2 suggested integrating a surface hydrodynamic model alongside the SWMM model to better capture urban flood dynamics. E1 and E3 recommended incorporating an optimization framework that systematically evaluates all potential modification strategies and automatically recommends solutions for enhanced decision support.

VI. Discussion

Significance. To the best of our knowledge, DrainScope is the first visual analytics system designed for analyzing urban drainage systems. It advances both drainage diagnostics and visual analytics in complex urban environments by bridging physically-based simulation models with explainable causal reasoning. Existing tools, such as SWMM and InfoWorks ICM, primarily produce numerical outputs and static reports, requiring experts to manually infer junction overflow causes [6]–[8]. In contrast, DrainScope encodes hydraulic dependencies in a drainage-oriented Sankey diagram, making local flow propagation and overflow causes more transparent. Unlike prior tools, it also supports interactive plan modification and iterative evaluation, with tracking and rollback. As demonstrated in our case studies, DrainScope uncovers cross-junction propagation patterns and hidden defects that existing tools miss, enabling more targeted and effective improvement strategies. Besides, the revised Samkey diagram enables analysts to interactively trace hydraulic dependencies within a physical, real-world drainage network. In this context, our work extends causal visualization concepts [30], [45], [62] to a domain characterized by physical and topological complexity.

Scalability. DrainScope shows potential for application in larger urban environments. First, urban drainage analysis is typically localized [63], [64]. Even in large cities, the causes of flooding during extreme events such as heavy rainfall are often confined to specific regions. It is uncommon for drainage failures occurring tens of kilometers away to affect a given location. City-wide disasters such as dam breaches typically exceed the capabilities of conventional drainage systems and fall outside the intended scope of this work. Second, our global-to-local visual analysis workflow enables users to identify and focus on critical regions. Starting from an overview of the entire drainage system, users can drill down

into relevant subsystems, aided by the automated sub-system extraction method and the drainage-oriented Sankey diagram. Third, to support scalability in larger settings, DrainScope can be integrated with simplified or parallel implementations of SWMM [65], [66], which improve simulation responsiveness. Finally, junction aggregation can further enhance both visual clarity and computational efficiency. For instance, merging neighboring junctions with similar hydraulic behavior, particularly those acting primarily as transit points such as *G60K009* and *G60R304* (Fig. $3B_2$), can reduce complexity without compromising analytical accuracy.

Lessons Learned. In interdisciplinary projects, differences in terminology, problem framing, and evaluation criteria can pose substantial communication barriers. We found it highly effective for visualization experts to gain domain knowledge through direct engagement, rather than relying solely on domain experts to articulate requirements. In particular, to facilitate interdisciplinary collaboration, we assigned visualization experts to work closely with domain teams, participating in their ongoing projects and tasks to gradually build up domain expertise. These hybrid team members, equipped with both visualization and domain expertise, played a critical role in aligning problem understanding, refining requirements, and validating prototypes. This approach reduced communication barriers and improved the efficiency of the design process.

Limitations and Future Work. Our work can be further improved in the following aspects:

Global Pattern Discovery in Urban Drainage Networks. DrainScope currently emphasizes detailed analysis of localized regions, with global insight limited to the visualization of overflow hotspots via color-encoded heatmaps in the map view. Future work will extend its capabilities to extract and summarize global patterns, including spatially recurrent failures and structurally similar subnetworks. To this end, we plan to compute overflow frequencies across historical simulations to identify persistently vulnerable regions, and apply graph mining techniques, such as motif detection and subgraph matching, to reveal common structural patterns associated with overflow. These extracted patterns can then be proactively recommended to users as high-priority regions or components for further diagnosis and planning.

Scalable Management of Improvement Plans. Although DrainScope offers basic mechanisms for tracking, reverting, and comparing improvement plans, its support does not yet scale to scenarios involving many iteratively generated plans. The current linked-view design requires users to manually connect each plan's summary with its underlying modifications, which becomes increasingly inefficient as the number of plans grows. Future work will investigate more scalable representations for managing plan evolution. Promising directions include: (i) an analytical provenance view that captures branching, inheritance, and convergence among plans; (ii) compact visual summaries (e.g., glyph-based encodings) that reduce view switching and support rapid comparison; and (iii) hierarchical abstractions that aggregate component-level changes into higher-level semantic groups, enabling analysis at multiple levels of granularity.

Automated Generation of Improvement Plans. Currently, DrainScope relies on an expert-driven trial-and-error approach for system improvement, which could be time-consuming and labor-intensive. In the future, we plan to integrate combinatorial optimization and multi-objective decision-making frameworks to automate the generation of improvement plans. This entails two main challenges: (1) handling complex interdependencies, as modifying one junction may affect others, and (2) balancing competing objectives such as overflow reduction, cost-efficiency, and long-term resilience. Tackling these challenges requires advances in optimization techniques and deeper integration of domain knowledge.

VII. Conclusion

Through close collaboration with domain experts, we characterize the domain problem of urban drainage system analysis and derive requirements. To satisfy the requirements, we develop a visual analytics approach named DrainScope, which assists experts in effectively identifying overflow-prone junctions, reasoning the root causes of overflows, and improving the drainage system. A novel drainage-oriented Sankey diagram is integrated into DrainScope to visualize the drainage process within the topographic and drainage topological context for overflow causality reasoning. A case study on a real-world drainage system, along with positive expert feedback, validates the effectiveness of DrainScope. This work establishes a foundation for future advancements in visual analytics for urban drainage systems and flood management.

References

[1] P. Stott, "How climate change affects extreme weather events," *Science*, vol. 352, no. 6293, pp. 1517–1518, 2016.

[2] L. Yang, Y. Yang, Y. Shen, J. Yang, G. Zheng, J. Smith, and D. Niyogi, "Urban development pattern's influence on extreme rainfall occurrences," *Nature Communications*, vol. 15, no. 1, p. 3997, 2024.

[3] F. Piadeh, K. Behzadian, and A. M. Alani, "A critical review of real-time modelling of flood forecasting in urban drainage systems," *J. Hydrol.*, vol. 607, p. 127476, 2022.

[4] B. Azari and M. Tabesh, "Urban storm water drainage system optimization using a sustainability index and LID/BMPs," *Sustainable Cities and Society*, vol. 76, p. 103500, 2022.

[5] A. E. Bakhshipour, U. Dittmer, A. Haghighi, and W. Nowak, "Toward sustainable urban drainage infrastructure planning: A combined multiobjective optimization and multicriteria decision-making platform," *Journal of Water Resources Planning and Management*, vol. 147, no. 8, p. 04021049, 2021.

[6] A. Elliott and S. A. Trowsdale, "A review of models for low impact urban stormwater drainage," *Environmental modelling & software*, vol. 22, no. 3, pp. 394–405, 2007.

[7] C. Zoppou, "Review of urban storm water models," *Environmental Modelling & Software*, vol. 16, no. 3, pp. 195–231, 2001.

[8] S. H. Kwon and J. H. Kim, "Machine learning and urban drainage systems: State-of-the-art review," *Water*, vol. 13, no. 24, p. 3545, 2021.

[9] D. S. Bisht, C. Chatterjee, S. Kalakoti, P. Upadhyay, M. Sahoo, and A. Panda, "Modeling urban floods and drainage using SWMM and MIKE URBAN: A case study," *Natural Hazards*, vol. 84, pp. 749–776, 2016.

[10] Y. Bai, N. Zhao, R. Zhang, and X. Zeng, "Storm water management of low impact development in urban areas based on SWMM," *Water*, vol. 11, no. 1, p. 33, 2018.

[11] T.-J. Chang, C.-H. Wang, and A. S. Chen, "A novel approach to model dynamic flow interactions between storm sewer system and overland surface for different land covers in urban areas," *J. Hydrol.*, vol. 524, pp. 662–679, 2015.

[12] K. Khatooni, F. Hooshyaripor, B. MalekMohammadi, and R. Noori, "A new approach for urban flood risk assessment using coupled SWMM–HEC-RAS-2D model," *J. Environ. Manag.*, vol. 374, p. 123849, 2025.

[13] A. M. Rabori and R. Ghazavi, "Urban flood estimation and evaluation of the performance of an urban drainage system in a semi-arid urban area using SWMM," *Water Environment Research*, vol. 90, no. 12, pp. 2075–2082, 2018.

[14] C. Montalvo, J. D. Reyes-Silva, E. Sañudo, L. Cea, and J. Puertas, "Urban pluvial flood modelling in the absence of sewer drainage network data: A physics-based approach," *J. Hydrol.*, vol. 634, p. 131043, 2024.

[15] L. M. Sidek, A. S. Jaafar, W. H. A. W. A. Majid, H. Basri, M. Marufuzzaman, M. M. Fared, and W. C. Moon, "High-resolution hydrological-hydraulic modeling of urban floods using infoworks ICM," *Sustainability*, vol. 13, no. 18, p. 10259, 2021.

[16] H. Wei, H. Wu, L. Zhang, and J. Liu, "Urban flooding simulation and flood risk assessment based on the InfoWorks ICM model: A case study of the urban inland rivers in zhengzhou, china," *Water Science & Technology*, vol. 90, no. 4, pp. 1338–1358, 2024.

[17] S. Boughandjioua, F. Laouacheria, and N. Azizi, "Machine learning algorithms investigation for urban drainage decision systems: Overview," in *Proceedings of IEEE DASA*, 2023, pp. 306–313.

[18] H. Hosseiny, F. Nazari, V. Smith, and C. Nataraj, "A framework for modeling flood depth using a hybrid of hydraulics and machine learning," *Scientific Reports*, vol. 10, p. 8222, 2020.

[19] X. Yin, Y. Chen, A. Bouferguene, H. Zaman, M. Al-Hussein, and L. Kurach, "A deep learning-based framework for an automated defect detection system for sewer pipes," *Automation in construction*, vol. 109, p. 102967, 2020.

[20] J. Noymanee and T. Theeramunkong, "Flood forecasting with machine learning technique on hydrological modeling," *Procedia Computer Science*, vol. 156, pp. 377–386, 2019.

[21] G. Zhi, Z. Liao, W. Tian, X. Wang, and J. Chen, "A 3d dynamic visualization method coupled with an urban drainage model," *J. Hydrol.*, vol. 577, p. 123988, 2019.

[22] G. Zhi, Z. Liao, W. Tian, and J. Wu, "Urban flood risk assessment and analysis with a 3d visualization method coupling the pp-pso algorithm and building data," *J. Environ. Manag.*, vol. 268, p. 110521, 2020.

[23] Z. Deng, S. Chen, X. Xie, G. Sun, M. Xu, D. Weng, and Y. Wu, "Multilevel visual analysis of aggregate geo-networks," *IEEE Trans. Vis. Comput. Graph.*, vol. 30, no. 7, pp. 3135–3150, 2024.

[24] G. Moreira, M. Hosseini, M. N. A. Nipu, M. Lage, N. Ferreira, and F. Miranda, "The urban toolkit: A grammar-based framework for urban visual analytics," *IEEE Trans. Vis. Comput. Graph.*, vol. 30, no. 1, pp. 1402–1412, 2024.

[25] G. Moreira, M. Hosseini, C. V. F. de Souza, L. Alexandre, N. Colaninno, D. de Oliveira, N. Ferreira, M. Lage, and F. Miranda, "Curio: A dataflow-based framework for collaborative urban visual analytics," *IEEE Trans. Vis. Comput. Graph.*, vol. 31, no. 1, pp. 1224–1234, 2025.

[26] Z. Deng, Y. Liu, M. Zhu, D. Xiang, H. Yu, Z. Su, Q. Lu, T. Schreck, and Y. Cai, "TraSculptor: Visual analytics for enhanced decision-making in road traffic planning," *IEEE Trans. Vis. Comput. Graph.*, pp. 1–16, 2025.

[27] Z. Deng, S. Chen, T. Schreck, D. Deng, T. Tang, M. Xu, D. Weng, and Y. Wu, "Visualizing large-scale spatial time series with GeoChron," *IEEE Trans. Vis. Comput. Graph.*, vol. 30, no. 1, pp. 1194–1204, 2024.

[28] N. Ferreira, M. Lage, H. Doraiswamy, H. T. Vo, L. Wilson, H. Werner, M. Park, and C. T. Silva, "Urbane: A 3D framework to support data driven decision making in urban development," in *Proceedings of IEEE VAST*, 2015, pp. 97–104.

[29] L. Chen, H. Wang, Y. Ouyang, Y. Zhou, N. Wang, and Q. Li, "FSLens: A visual analytics approach to evaluating and optimizing the spatial layout of fire stations," *IEEE Trans. Vis. Comput. Graph.*, vol. 30, no. 1, pp. 847–857, 2024.

[30] Z. Deng, D. Weng, X. Xie, J. Bao, Y. Zheng, M. Xu, W. Chen, and Y. Wu, "Compass: Towards better causal analysis of urban time series," *IEEE Trans. Vis. Comput. Graph.*, vol. 28, no. 1, pp. 1051–1061, 2022.

[31] N. Ferreira, J. Poco, H. T. Vo, J. Freire, and C. T. Silva, "Visual exploration of big spatio-temporal urban data: A study of New York City taxi trips," *IEEE Trans. Vis. Comput. Graph.*, vol. 19, no. 12, pp. 2149–2158, 2013.

[32] Y. Wu, D. Weng, Z. Deng, J. Bao, M. Xu, Z. Wang, Y. Zheng, Z. Ding, and W. Chen, "Towards better detection and analysis of massive spatiotemporal co-occurrence patterns," *IEEE Trans. Intell. Transp. Syst.*, vol. 22, no. 6, pp. 3387–3402, 2021.

[33] A. Malik, R. Maciejewski, N. Elmqvist, Y. Jang, D. S. Ebert, and W. K. Huang, "A correlative analysis process in a visual analytics environment," in *Proceedings of IEEE VAST*, 2012, pp. 33–42.

[34] J. Chen, Q. Huang, C. Wang, and C. Li, "SenseMap: Urban performance visualization and analytics via semantic textual similarity," *IEEE Trans. Vis. Comput. Graph.*, vol. 30, no. 9, pp. 6275–6290, 2024.

[35] X. Huang, Y. Zhao, C. Ma, J. Yang, X. Ye, and C. Zhang, "TrajGraph: A graph-based visual analytics approach to studying urban network centralities using taxi trajectory data," *IEEE Trans. Vis. Comput. Graph.*, vol. 22, no. 1, pp. 160–169, 2016.

[36] L. Styve, C. Navarra, J. M. Petersen, T.-S. Neset, and K. Vrotsou, "A visual analytics pipeline for the identification and exploration of extreme weather events from social media data," *Climate*, vol. 10, no. 11, p. 174, 2022.

[37] Z. Deng, H. Chen, Q.-L. Lu, Z. Su, T. Schreck, J. Bao, and Y. Cai, "Visual comparative analytics of multimodal transportation," *Visual Informatics*, vol. 9, no. 1, pp. 18–30, 2025.

[38] G. G. Zanabria, M. M. Raimundo, J. Poco, M. B. Nery, C. T. Silva, S. Adorno, and L. G. Nonato, "CriPAV: Street-level crime patterns analysis and visualization," *IEEE Trans. Vis. Comput. Graph.*, vol. 28, no. 12, pp. 4000–4015, 2022.

[39] N. Cao, C. Lin, Q. Zhu, Y. Lin, X. Teng, and X. Wen, "Voila: Visual anomaly detection and monitoring with streaming spatiotemporal data," *IEEE Trans. Vis. Comput. Graph.*, vol. 24, no. 1, pp. 23–33, 2018.

[40] S. Rauer-Zechmeister, D. Cornel, B. Sadransky, Z. Horváth, A. Konev, A. Buttinger-Kreuzhuber, R. Heidrich, G. Blöschl, E. Gröller, and J. Waser, "HORA 3D: Personalized flood risk visualization as an interactive web service," *Comput. Graph. Forum*, vol. 43, no. 3, 2024.

[41] D. Cornel, A. Buttinger-Kreuzhuber, A. Konev, Z. Horváth, M. Wimmer, R. Heidrich, and J. Waser, "Interactive visualization of flood and heavy rain simulations," *Comput. Graph. Forum*, vol. 38, no. 3, pp. 25–39, 2019.

[42] Z. Deng, D. Weng, Y. Liang, J. Bao, Y. Zheng, T. Schreck, M. Xu, and Y. Wu, "Visual cascade analytics of large-scale spatiotemporal data," *IEEE Trans. Vis. Comput. Graph.*, vol. 28, no. 6, pp. 2486–2499, 2022.

[43] Z. Deng, D. Weng, J. Chen, R. Liu, Z. Wang, J. Bao, Y. Zheng, and Y. Wu, "Airvis: Visual analytics of air pollution propagation," *IEEE Trans. Vis. Comput. Graph.*, vol. 26, no. 1, pp. 800–810, 2020.

[44] C. Jung, S. Yim, G. Park, S. Oh, and Y. Jang, "CATOM: Causal topology map for spatiotemporal traffic analysis with granger causality in urban areas," *IEEE Trans. Vis. Comput. Graph.*, no. 01, pp. 1–16, Oct. 5555.

[45] M. Pi, H. Yeon, H. Son, and Y. Jang, "Visual cause analytics for traffic congestion," *IEEE Trans. Vis. Comput. Graph.*, vol. 27, no. 3, pp. 2186–2201, 2021.

[46] Z. Deng, D. Weng, and Y. Wu, "You are experienced: Interactive tour planning with crowdsourcing tour data from web," *J. Vis.*, vol. 26, no. 2, pp. 385–401, 2023.

[47] G. D. Lorenzo, M. L. Sbodio, F. Calabrese, M. Berlingerio, F. Pinelli, and R. Nair, "AllAboard: Visual exploration of cellphone mobility data to optimise public transport," *IEEE Trans. Vis. Comput. Graph.*, vol. 22, no. 2, pp. 1036–1050, 2016.

[48] Q. Q. Liu, Q. Li, C. F. Tang, H. Lin, X. Ma, and T. Chen, "A visual analytics approach to scheduling customized shuttle buses via perceiving passengers' travel demands," in *Proceedings of IEEE Visualization Conference - Short Papers*, 2020, pp. 76–80.

[49] D. Weng, R. Chen, Z. Deng, F. Wu, J. Chen, and Y. Wu, "Srvis: Towards better spatial integration in ranking visualization," *IEEE Trans. Vis. Comput. Graph.*, vol. 25, no. 1, pp. 459–469, 2019.

[50] Q. Li, Q. Liu, C. Tang, Z. W. Li, S. C. Wei, X. R. Peng, M. H. Zheng, T. Chen, and Q. Yang, "Warehouse Vis: A visual analytics approach to facilitating warehouse location selection for business districts," *Comput. Graph. Forum*, vol. 39, no. 3, pp. 483–495, 2020.

[51] D. Weng, C. Zheng, Z. Deng, M. Ma, J. Bao, Y. Zheng, M. Xu, and Y. Wu, "Towards better bus networks: A visual analytics approach," *IEEE Trans. Vis. Comput. Graph.*, vol. 27, no. 2, pp. 817–827, 2021.

[52] D. Liu, D. Weng, Y. Li, J. Bao, Y. Zheng, H. Qu, and Y. Wu, "SmartAdP: Visual analytics of large-scale taxi trajectories for selecting billboard locations," *IEEE Trans. Vis. Comput. Graph.*, vol. 23, no. 1, pp. 1–10, 2017.

[53] Y. Zhang, L. Xu, S. Tao, Q. Guan, Q. Li, and H. Zeng, "Cslens: Towards better deploying charging stations via visual analytics - a coupled networks perspective," *IEEE Trans. Vis. Comput. Graph.*, vol. 31, no. 1, pp. 251–261, 2025.

[54] H. Ribicic, J. Waser, R. Fuchs, G. Blöschl, and M. E. Gröller, "Visual analysis and steering of flooding simulations," *IEEE Trans. Vis. Comput. Graph.*, vol. 19, no. 6, pp. 1062–1075, 2013.

[55] J. Waser, H. Ribicic, R. Fuchs, C. Hirsch, B. Schindler, G. Blöschl, and M. E. Gröller, "Nodes on ropes: A comprehensive data and control flow for steering ensemble simulations," *IEEE Trans. Vis. Comput. Graph.*, vol. 17, no. 12, pp. 1872–1881, 2011.

[56] M. Sedlmair, M. D. Meyer, and T. Munzner, "Design study methodology: Reflections from the trenches and the stacks," *IEEE Trans. Vis. Comput. Graph.*, vol. 18, no. 12, pp. 2431–2440, 2012.

[57] H. A. Simon, "The new science of management decision," 1960.
[58] B. Shneiderman, "The eyes have it: A task by data type taxonomy for information visualizations," in *The craft of information visualization*. Elsevier, 2003, pp. 364–371.
[59] K. Sugiyama, S. Tagawa, and M. Toda, "Methods for visual understanding of hierarchical system structures," *IEEE Trans. Syst. Man Cybern.*, vol. 11, no. 2, pp. 109–125, 1981.
[60] M. Gleicher, D. Albers, R. Walker, I. Jusufi, C. D. Hansen, and J. C. Roberts, "Visual comparison for information visualization," *Information Visualization*, vol. 10, no. 4, pp. 289–309, 2011.
[61] A. N. Pedersen, J. W. Pedersen, A. Vigueras-Rodriguez, A. Brink-Kjær, M. Borup, and P. S. Mikkelsen, "The bellinge data set: Open data and models for community-wide urban drainage systems research," *Earth System Science Data Discussions*, vol. 2021, pp. 1–28, 2021.
[62] J. Bae, T. Helldin, and M. Riveiro, "Understanding indirect causal relationships in node-link graphs," *Comput. Graph. Forum*, vol. 36, no. 3, pp. 411–421, 2017.
[63] S. N. Mugume, D. E. Gomez, G. Fu, R. Farmani, and D. Butler, "A global analysis approach for investigating structural resilience in urban drainage systems," *Water Research*, vol. 81, pp. 15–26, 2015.
[64] K.-H. Wang and A. Altunkaynak, "Comparative case study of rainfall-runoff modeling between swmm and fuzzy logic approach," *Journal of Hydrologic Engineering*, vol. 17, no. 2, pp. 283–291, 2012.
[65] A. Farina, A. Di Nardo, R. Gargano, J. A. van der Werf, and R. Greco, "A simplified approach for the hydrological simulation of urban drainage systems with swmm," *J. Hydrol.*, vol. 623, p. 129757, 2023.
[66] G. Burger, R. Sitzenfrei, M. Kleidorfer, and W. Rauch, "Parallel flow routing in SWMM 5," *Environmental Modelling & Software*, vol. 53, pp. 27–34, 2014.

Mingwei Lin is a graduate student at the School of Software Engineering, South China University of Technology, and his research interests are data visualization, visual analytics, and urban computing.

Zikun Deng is a tenure-track associate professor at School of Software Engineering, South China University of Technology. He received his Ph.D. degree in Computer Science from the State Key Lab of CAD&CG, Zhejiang University in 2023. His research interests mainly include visual analytics, visualization, data mining, and their application in smart city, industry 4.0, and digital twins. He has published more than 10 papers in IEEE TVCG. For more information, please visit https://zkdeng.org.

Qin Huang received his bachelor's degree from the School of Software Engineering, South China University of Technology in 2025, and his research interests are data visualization and visual analytics.

Yiyi Ma is a researcher and doctoral supervisor of the Hundred Talents Program of the Institute of Municipal Engineering, School of Architecture and Engineering, Zhejiang University. Her main research interests are urban drainage, including water-gas and water-sand two-phase flow in pipelines, urban storm-water disaster prevention and control, etc. She has published more than 20 papers in internationally renowned journals such as Journal of Hydraulic Engineering (ASCE) and Journal of Engineering Mechanics (ASCE).

Lin-Ping Yuan is a research assistant professor in the Department of Computer Science and Engineering at the Hong Kong University of Science and Technology. Her research interests lie in the intersection of virtual/augmented reality (VR/AR), human-computer interaction (HCI), and data visualization (VIS).

Jie Bao got his Ph.D degree in Computer Science from University of Minnesota at Twin Cities in 2014. He worked as a researcher in Urban Computing Group at MSR Asia from 2014 to 2017. He currently leads the Data Platform Division in JD Urban Computing Business Unit. His research interests include: Spatio-temporal Data Management/Mining, Urban Computing, and Location-based Services.

Yu Zheng is a Vice President and Chief Data Scientist at JD Tech., passionate about using big data and AI technology to tackle urban challenges. His research interests include big data analytics, spatio-temporal data mining, machine learning, and artificial intelligence. He also leads the JD Urban Computing Business Unit as the president and serves as the director of the JD Intelligent City Research. Before joining JD, he was a senior research manager at Microsoft Research. Zheng is also a Chair Professor at Shanghai Jiao Tong University, an Adjunct Professor at Hong Kong University of Science and Technology.

Yi Cai is the Dean of School of Software Engineering in South China University of Technology, the Director of The China Ministry of Education Key Laboratory of Big Data and Robotic Intelligence. He had received his PhD degree in the Chinese University of Hong Kong, and work as postdoctoral fellow in City University of Hong Kong. He has published more than 170 high quality papers in top journals and conferences such as IEEE TVCG, TKDE, TMM, AAAI, ACL, and ACM MM. He also has published 2 academic monographs and acts as the Chairman and Program Committee members of more than 20 prestigious international academic conferences.